Meteorol Atmos Phys 102, 223–241 (2008)
DOI 10.1007/s00703-008-0329-0
Printed in The Netherlands

Meteorology and Atmospheric Physics

[1] GAME/CNRM, Météo-France, CNRS, Paris, France
[2] FAOFA Vigo University, Ourense, Spain

Urban-breeze circulation during the CAPITOUL experiment: observational data analysis approach

J. Hidalgo[1,2], **G. Pigeon**[1], **V. Masson**[1]

With 10 Figures

Received 10 May 2007; Accepted 18 June 2008
Published online 4 December 2008

Summary

An experimental study focused on the urban-breeze circulation observed in Toulouse, South-West of France, during the Intensive Observation Period number 5 (IOP5, 3rd and 4th July 2004) of the CAPITOUL experiment (Feb. 2004 to Feb. 2005) is presented. The influence of the urban breeze circulation on the structure and the dynamics of the Atmospheric Boundary Layer is analysed by using ground stations, wind profilers (UHF radar), radio soundings and aircraft data. The IOP5 is a summertime anticyclonic situation with low wind, strong insulation and a deep boundary layer with a sheared wind profile.

The temporal and spatial relationship between the Surface Energy Balance (SEB), the diurnal evolution of the surface temperature and the dynamics of the airflow within the mixed layer are studied for urban and rural sites. The vertical and horizontal structure of the urban heat island are analysed from both surface stations and aircraft data. The nocturnal urban heat island reaches 5 °C. In the early morning, the city air becomes 1 °C cooler than in the countryside (due to efficient heat storage and building shade on the city urban canopy), then warmer again (1 °C) in the afternoon, due to negligible evaporation and strong sensible heat flux in the city. The daytime heat island is also present in altitude, being localized above the city centre at 350 m of height (1 °C) and advected to leeward at 1100 m of height (0.5 °C).

This diurnal heat island is associated to an urban-breeze circulation characterized by a surface convergence towards the city at low levels and a divergence in upper boundary layer. The urban breeze grows in intensity from 2 m s^{-1} (at 12.00 UTC) to 5–6 m s^{-1} (at 18.00 UTC). Aircraft measurements show that the urban breeze horizontal extension is 2 to 3 times larger than the city size.

Correspondence: Julia Hidalgo, FT2DC, Atmospheric Physics Area, University of Vigo, Ed. de Fisicas, As Lagoas, 32004 Ourense, Spain (E-mail: julia.hidalgo@uvigo.es, jhidalgo@labein.es)

1. Introduction

The urban-breeze is a mesoscale phenomenon (Oke 2005) characterized by a surface convergent flow from the countryside to the city centre, induced by a horizontal temperature gradient. This dynamical circulation at low levels is completed by a divergent flow at the top of the Atmospheric Boundary Layer (ABL).

Urban-breeze is defined theoretically by analogy with the sea-breeze circulation in coastal environments. The sea-breeze is a well documented mesoscale flow caused by unequal land-sea diurnal heating cycle that blows from the sea to the land due to this differential heating. The horizontal structure is characterized by the land surface warmer than the sea surface with a maximum gradient in the late afternoon. Warmer air rises over the land and a local onshore circulation starts, with colder air from the sea being drawn in over the land. At the same time, due to the thermally induced horizontal pressure gradient, the ascending air returns seaward as the upper

return current. Its vertical extension is generally restricted to the lowest 1–2 km of the atmosphere, therefore the sea breeze is strongly influenced by the boundary layer processes. In coastal cities this phenomenon has a strong influence on the urban boundary layer and has been well documented (Fisher 1960; Walsh 1974; Atkinson 1981; Rotunno 1983; Nakane and Sasano 1986; Niino 1987; Feliks 1994; Finkele et al. 1995; Lemonsu et al. 2004, 2006a, b; Augustin et al. 2006). They explore its properties and structure, its dynamics and its overall impact on the air quality of coastal cities. However, few is known on the dynamics and structure of the urban-breeze circulation in an inland city. Only one study (Wong and Dirks 1978) analyses urban thermally induced motions using observational data for an inland city. It shows a convergence towards the city at low level in the boundary layer over St. Louis using aircraft data from the METROMEX campaign (Changnon 1981).

The different responses of the land surface and the urbanized surface to the diurnal cycle create the Urban Heat Island (UHI), which is the source of the urban-breeze circulation. The UHI is easily detectable by a meteorological surface network with a good horizontal distribution. However, to describe the urban-breeze it is necessary to characterize other effects, like the convergent flow of air toward the city centre, which can not be measured easily using standard equipment. For this, numerical simulations are used by Lemonsu and Masson (2002) as a strategy to study this phenomenon and to quantify the unmeasured 3-D mesoscale urban effects.

Urban-breeze can affect the transfer of pollution from interurban industrial areas into the city centre. A better understanding of these breeze circulations is of primary importance in the prediction of pollution peaks and the evaluation of air quality policy in the cities. Furthermore under moist conditions the urban breeze thermodynamics can provide a favourable environment for convective thunderstorm over the urban area and precipitation downwind resulting in more lightning activity and heavier precipitations. Shepherd (2005) provides a concise review of recent (1990–present) studies related to how the urban environment affects precipitation.

During the CAPITOUL experiment, meteorological conditions and thermo-dynamical properties were provided by different instruments that supplied complementary space and time information. This allows us to study both, the horizontal ground characteristics and the 3D properties of the breeze, using wind profilers, radio soundings and aircraft data.

The work presented in this paper is an experimental study focused on the urban-breeze circulation observed in the city of Toulouse, in the South-West of France, during the Intensive Observation Period number 5 (IOP5, 3rd and 4th July 2004) of the CAPITOUL experiment (Feb. 2004 to Feb. 2005, Masson et al. 2008). The analyse focuses on the city influence on the structure and the dynamics of the ABL. The IOP5 corresponds to a summertime anticyclonic situation with low wind and high insulation, meteorological conditions which are favourable to breezes episodes.

2. Observational network

The Canopy and Aerosol Particles Interaction in Toulouse Urban Layer (CAPITOUL) experiment took place over the city of Toulouse, France, from February 2004 to February 2005. In this context, 15 IOPs were carried out during a year to characterize the diverse interactions (thermodynamically and chemically) between the city and the atmosphere under a wide range of meteorological conditions. An extensive description is presented in Masson et al. (2008).

The CAPITOUL experiment had a broad experimental deployment in urban and rural zones, providing boundary layer characteristics for both environments. For this study, ground stations, a wind profiler (Ultra-High Frequency (UHF) radar), radio soundings and aircraft data are used.

2.1 Surface network in the area of study

The surface network was placed in different Urban Climate Zones (UCZ) according to recommendations of Oke (2005) and was composed of (Fig. 1):

– An assembly of 21 light stations recording temperature and relative humidity with 12 min sampling, situated in the city centre and in the suburban areas of Toulouse.
– A network of synoptical ground stations of Meteo-France measured the horizontal wind

velocities at a height of 10 m. The temperature and relative humidity levels were recorded at a height of 2 m in a 10 km radius from the city centre.

– An instrumented pneumatic tower situated on the old core of the city is considered as the reference station chosen to describe the properties of the city centre of Toulouse. This central tower, which is 30 m high, was situated on the roof of a building (situated 20 m above the ground). Temperature, relative humidity, wind speed, pressure, upward and downward global short- and long-wave radiation, and the turbulent fluxes measurements were recorded. The turbulent fluxes are computed on 30 min period with eddy covariance techniques.
– In addition, measurements of the Surface Energy Balance (SEB) (measurements of radia-

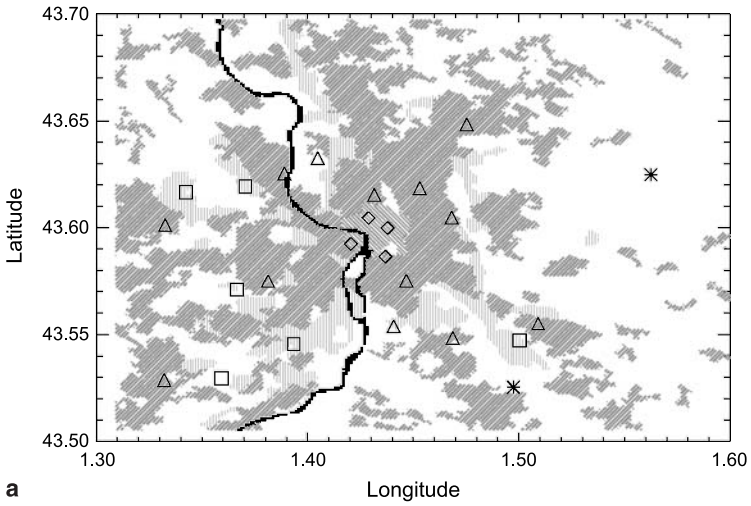

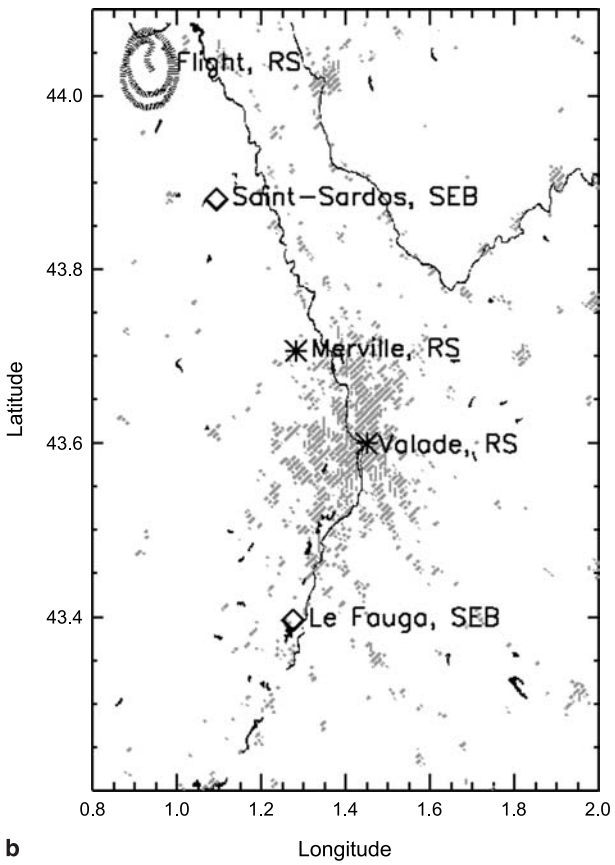

Fig. 1a. Surface network emplacement. The diamonds, triangles, squares and asterisks corresponds to urban, residential, non-residential and rural zones, respectively described in Table 1. The covers are from the Corine Land Cover database: urban zone (grey (135°)), suburban zone (grey (45°)), commercial areas (grey (90°)) and the Garonne river (in black). (**b**) Radio sounding sites and SEB stations emplacement

tion + turbulent fluxes) with a 30 min sampling were also recorded using two flux stations situated for the first one at 15 km south-west (Fauga, situated in a grassland area) and for the second one at 40 km north-west of Toulouse (Saint-Sardos, situated in a irrigated maize crop). The stations were equipped with the same instrumentation as the central site. Both types of covers are common around Toulouse area.

The urban stations surroundings are described using a 100 m resolution urban database produced from 0.25 m resolution aerial ortho-rectified photography and a 2D and 3D vectorial database. A semi-automatic classification (GRASS 6.0, Open Source GIS) is applied on the photography to separate the environment into four surface categories: high vegetation, low vegetation, roofs and roads. The sky view factor is calculated for each station from a hemispheric picture. The surface network characteristics and emplacement are shown in Table 1 and Fig. 1.

Owing to this data base and to the sky view factor, four classes of urbanization are chosen: urban area, residential suburban area, non-residential suburban area and rural area.

Table 1. Surface network characteristics: station number, longitude (°E), latitude (°N), altitude over the sea level (m), distance from the central tower (m) (station 27, considered as the city centre reference), sky view factor, aspect ratio, percent of built cover in a radius of 500 m, roughness class according to the Davenport (2000) classification, height of measure for the four classes defined (m) (urban area (UA), residential suburban area (RSUA), non-residential suburban area (NRSUA) and rural area (RA), respectively)

Station	LON	LAT	ALT	X	Fvc	AR	% Built	UCZ	H
UA									
27	1.4453	43.6036	144	0			100	2	20 + 30
21	1.4279	43.5962	138	1624	0.33	1.34	90	2	6
12	1.4443	43.5902	140	1493	0.23	2.03	80	2	6
07	1.4363	43.6083	139	894	0.54	0.65	80	3	6
RSUA									
01	1.4827	43.6522	143	6189	0.68	0.39	70	5	6
02	1.4122	43.6364	131	4524	0.82	0.19	0	6	6
04	1.4605	43.6224	145	2427	0.47	0.83	90	3	6
05	1.4389	43.6192	138	1810	0.45	0.9	60	3	6
08	1.3400	43.6050	180	8502	0.54	0.65	70	5	6
09	1.4757	43.6085	147	2514	0.61	0.51	70	3	6
10	1.4367	43.5888	138	1788	0.3	1.49	90		6
11	1.3886	43.5788	156	5342	0.58	0.58	50	5	6
13	1.4541	43.5791	150	2814	0.51	0.73	60	3	6
14	1.5165	43.5589	151	7595	0.53	0.67	60	5	6
15	1.4482	43.5577	260	5103	0.69	0.41	0	7	6
17	1.4762	43.5521	151	6244	0.6	0.52	70	5	6
19–20	1.3396	43.5326	167	11624	0.6	0.53	40	5	6
03	1.3964	43.6291	140	4860	0.6	0.52	60	5	6
NRSUA									
06	1.3498	43.6203	153	7928	0.79	0.24	20	6	6
16	1.4009	43.5493	148	7016	0.79	0.24	70	4	6
18	1.5077	43.5510	145	7712			90	4	3 + 4
22	1.3780	43.6230	151	5846			100	4	2.10
23	1.3667	43.5333	163	10067			80	6	2.10
24	1.3740	43.5747	158	6589			70	6	2.10
RA									
25	1.5049	43.5291	148	9570			10	6	2.10
26	1.5699	43.6286	207	10435			10	7	2.10

2.2 Boundary layer Instrumentation

The study uses observations collected by radio soundings, UHF-band wind profiler, and an instrumented aircraft. This allowed a quasi-continuous remote monitoring of the boundary layer and of the low troposphere during the two days of the IOP.

- Two sites were equipped with radio sounding systems. One located at Merville, a rural zone situated at approximately 15 km north-west of the city centre. The second one, the Valade's site, was situated in Toulouse's city centre. Radio soundings were performed four times per day at 03.30, 08.00, 13.00 and 18.00 UTC.
- The DEGREWIND PCL1300 wind profiler was situated in the city centre at 100 m of the central tower. Measures of radar reflectivity, wind force, wind direction and its vertical velocity were registered with a 75 m vertical resolution, 4000 m vertical coverage and 6 min temporal resolution. Radar data were compared with the vertical wind profiles from the radio sounding in the city centre to validate the quality of the measurements.
- The Météo-France instrumented aircraft *Piper Aztec* performed two flights per day during this IOP (AZ0423 and AZ0424 on the 3rd July and AZ0425 and AZ0426 on the 4th July). Three horizontal flight legs were made over the city centre and the rural zones at an altitude of 350, 1100 and 1650 m. The following aircraft data set is used in this study: the potential temperature, the water vapour mixed ratio, the wind force and direction (the sampling period was 1 Hz which, given the speed of the plane, is equivalent to a spatial resolution of 70 m).

3. Meteorological context of this IOP

The study is focused on the thermal and the dynamical properties of the ABL for the 4th July 2004 over the city of Toulouse and its surrounding country. To improve the nocturnal process comprehension, for certain analyses, we extend the study to the 3rd July 2004.

The synoptic situation allowed the development of an anticyclone in the South of the country. A high pressure ridge, from the Atlantic Ocean to the North of Europe was present during the period of study. Toulouse was situated in a barometric marsh which evolved into a depresionary zone during the 5th July. The result of this stability was a very sunny period. The presence of a little Cumuli in the morning of the 3rd July, between 08.00 to 12.00 UTC, limits the fraction of insulation to 88%. The net radiation measured at the central tower at midday was 600 $W\,m^{-2}$. During the 4th July there were no clouds, the fraction of insulation for this day being of 91%. The period presents high thermal amplitude, particularly on the 4th July with a minimum temperature of 11 °C during night-time and a maximum of 34 °C.

The boundary layer wind was characterized by a weak velocity profile varying from 0.5 $m\,s^{-1}$ in the night of 3rd to 4th July to a maximum of 6 $m\,s^{-1}$ in the late afternoon of the 4th July. The wind was blowing from north-west on the 3rd July. The first change of the surface wind from north-west to the south-east was at 21.00 UTC. This creates a region of a weak flow in the transition layer between the south-easterly flow near the surface to the north-westerly flow at upper-levels (Fig. 2). A second change in the surface wind towards west occurred after 20.00 UTC on the 4th July, when a westerly air mass arrives over Toulouse. This change of direction in the mean flow is captured by the UHF radar, situated in the city centre, in the firsts 1500 m of the ABL (Fig. 2).

The 15 days preceding the experiment corresponded to a cloudy period with no rain, the accumulated precipitation was only 1 mm. As a consequence, there was no water available for evaporation on urban surfaces while the soil is still sufficiently moist to enable evapotranspiration by the vegetation. On the 4th July the specific humidity in the ABL had a constant value of 7 $g\,kg^{-1}$ until late afternoon. At 20.00 UTC the new westerly air mass induced an increase of the specific humidity to a maximum 10 $g\,kg^{-1}$ near the surface.

4. Temporal and spatial relations between thermodynamics fields and surface features

As described by Oke (1981, 1987), Unger et al. (2001) and Eliasson and Svensson (2003), the diurnal cycle and the horizontal pattern of temperature and moisture as well as the surface fluxes have a strong dependence on varied fac-

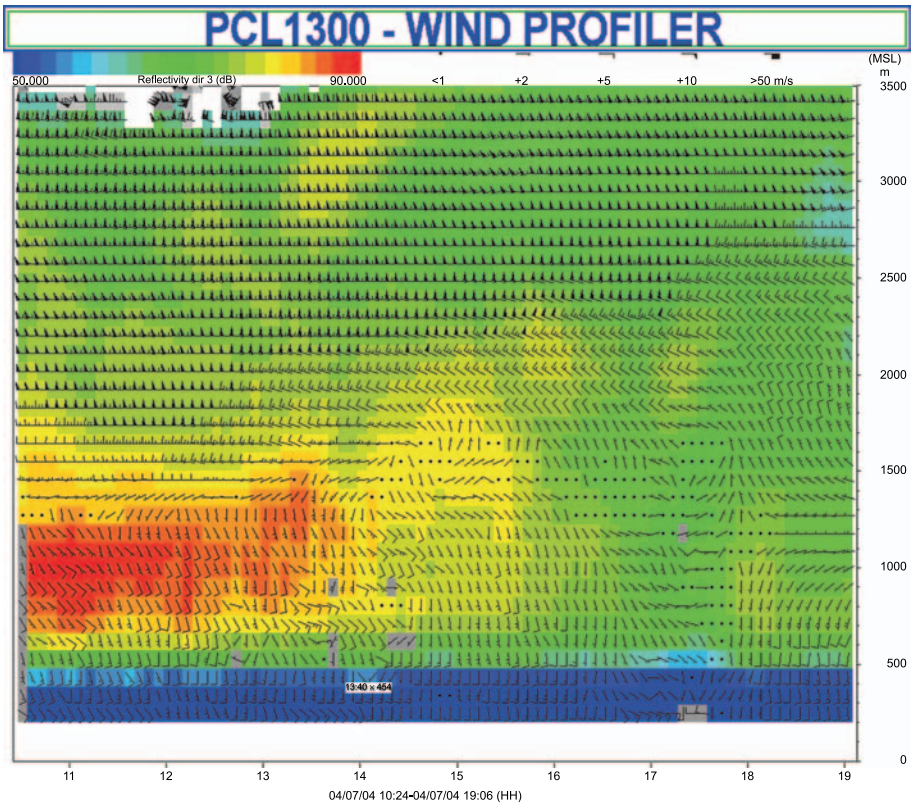

Fig. 2. Time-height cross-section of the horizontal wind superimposed to the radar reflectivity observed by the UHF radar the 4th July 2004

tors, such as for example: the surface geometry (aspect ratio, sky view-factor, roughness length and albedo), the properties of artificial materials in urban centres (urban cover fraction, moisture availability. . .) and the anthropogenic emissions. In this section, the spatial and temporal evolution of these thermodynamic fields are analysed for the 4th July 2004.

4.1 Surface Energy Balance (SEB)

The surface energy balance is significantly altered by urban areas (White et al. 1978; Grimmond and Oke 1999; Oke et al. 1999). The difference of SEB between the city and the rural zones affects the whole boundary layer, its stability, thermodynamic properties and the mixing layer height (Christen and Vogt 2004). The modified urban SEB is the UHI source, which is the key element of the urban-breeze circulation development.

During this IOP three experimental sites (two rural and one urban) computed the SEB on 30 min period. The measured turbulent flux densities are an area-averaged response of the surface. The urban site describes an integrated flux from an area representative of the local scale, 'urban neighbourhood' (10^4–$10^6\,\mathrm{m}^2$) (Christen and Vogt 2004). Thanks to the Toulouse homogeneity in terms of construction density, building type and materials, although it is a simplification, we will consider this value as representative for the entire city centre.

The energy balance at the top of the street canyon is described by Oke (1988) as

$$Q^* + Q_\mathrm{F} = Q_\mathrm{LE} + Q_\mathrm{H} + \Delta Q_\mathrm{s} + \Delta Q_\mathrm{A}$$

The flux densities of net all-wave radiation Q^*, upward sensible heat $Q_\mathrm{H} = \rho C_p \overline{w'\theta'}$ and upward latent heat $Q_\mathrm{LE} = \rho L_v \overline{w'q'}$ at the surface are directly measured. The latter two are calculated using the eddy-correlation method. Following Pigeon et al. (2007a), we can estimate the advection term (ΔQ_A) as

$$\int_0^{30} \rho C_p \bar{u} \frac{\partial T}{\partial x} dz$$

From the measurement network, $\bar{u} = 5\,\mathrm{m\,s}^{-1}$, $\Delta T = 1\mathrm{K}$ and $\Delta x = 10^4\,\mathrm{m}$. Consequently, $\Delta Q_\mathrm{A} = 6\,\mathrm{W\,m}^{-2}$ and can be ignored in the SEB considering the order of magnitude of the other fluxes.

Finally the sum of the heat storage (ΔQ_s, positive for warming) and the anthropogenic heat

flux (Q_F) is estimated from the residual of the budget as

$$R = \Delta Q_s - Q_F = Q^* - (Q_{LE} + Q_H)$$

The 4th July 2004 is a cloudless day at all sites (Fig. 3) with maximum net all-wave radiation Q^* of 600–650 W m^{-2} at 12.00 UTC (LT = local summer time = UTC + 2 h). The major differences of Q^* are present at night caused by the differences on the storage term for both sites. We assume that in summer, for the city of Toulouse (Pigeon et al. 2007b), the heat stored ΔQ_s is the dominant term of the residual component. The heat storage depends on materials nature and moist availability, for this reason urbanized areas and rural areas present thus different values of ΔQ_s.

This solar energy is distributed in the different terms of the energy balance. For the rural site Saint Sardos (Fig. 3b), during the night from 3rd to 4th July the sensible and the latent flux densities are zero until the sunshine. Radiative loss (Q^*) by infra-red radiation creates negative values of the residual term ($R = -40$ W m^{-2}, directed from the ground to the atmosphere). During the day the sensible heat flux increases fast in the morning with a maximum value of 150 W m^{-2} at 11.30 UTC, then decreases nearly to zero during the afternoon due to evaporation cooling. This rural site is situated in a maize crop irrigated during the afternoon. The latent flux Q_{LE} reaches its maximum value 500 W m^{-2} at 15.00 UTC. Sunset, around 18.00 UTC, creates a gradient of temperature as the atmosphere is hotter than the ground. Then, the sensible heat flux lowers and becomes negative reaching -50 W m^{-2} after 20.00 UTC.

Even at the Fauga site (Fig. 3c), which was non-irrigated grassland, Q_{LE} reaches a maximum of 220 W m^{-2} during the morning and Q_H has a

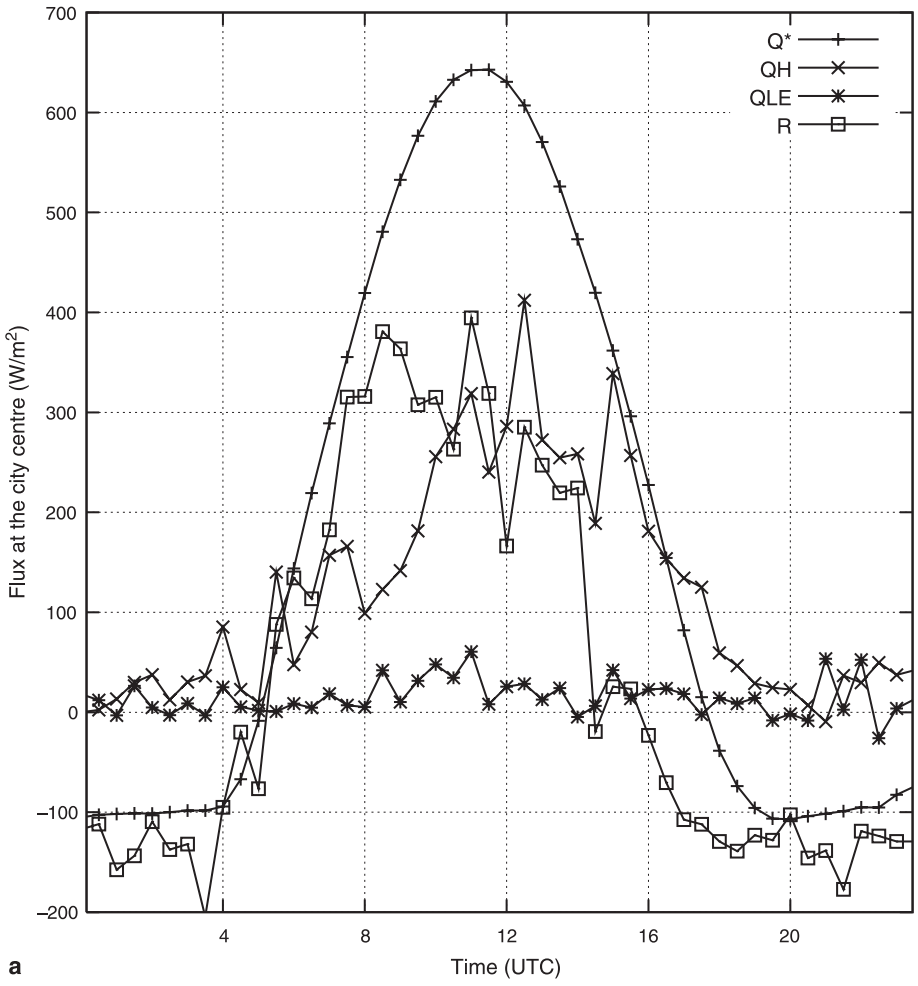

Fig. 3a, b. Energy balance components for the 4th July 2004 in the central tower (**a**) and in the rural sites (Saint Sardos, (**b**) and Fauga, (**c**). Flux densities of net all-wave radiation (Q^*), sensible heat (Q_H), latent heat (Q_{LE}) and the residual term calculated as $R = Q^* - (Q_{LE} + Q_H)$

constant value of $90\,W\,m^{-1}$ between 12.00 to 16.00 UTC decreasing to zero in late afternoon. The Bowen ratio is higher than 0.5 and indicates that the soil is moist.

In the city (Fig. 3a), during the night from 3rd to 4th July, the sensible flux density, in contrast to the rural sites, presents small positive values. During the afternoon, the sensible heat flux value reaches a mean value of $300\,W\,m^{-2}$. Mid-latitude cities with negligible vegetation and irrigation show less evapotranspiration than their surroundings and during this very sunny day, Q_{LE} remains lower than $50\,W\,m^{-2}$ which is very weak. This reduced daytime evapotranspiration (Q_{LE}) in the urban area results in increased magnitudes of sensible heat (Q_H) and heat storage in the construction materials (ΔQ_s) over the entire day. In the morning the heat is mainly stored in the urban fabric and is released as turbulent sensible heat into the atmosphere in the late afternoon and evening (Oke 1988).

To summarize, during the period of the breeze (12.00 to 18.00 UTC), the sensible heat flux in the rural sites is very weak (close to zero at Saint Sardos and $90\,W\,m^{-2}$ at Fauga) regardless of the surface cover (an irrigated maize crop land at Saint-Sardos and a grassland area at Fauga). The city centre presents strong Q_H positive values ($300\,W\,m^{-2}$) during the same period heating the air above the city and creating a positive anomaly of temperature between the city and the country, which is a key process of the urban-breeze circulation.

4.2 Urban heat island

Turbulent flux differences on Q_H and Q_{LE} between urban and rural zones produce the differences in the diurnal evolution of temperature and relative humidity. The diurnal cycle of rural and urban potential temperature at the surface is analysed in this section. The singular

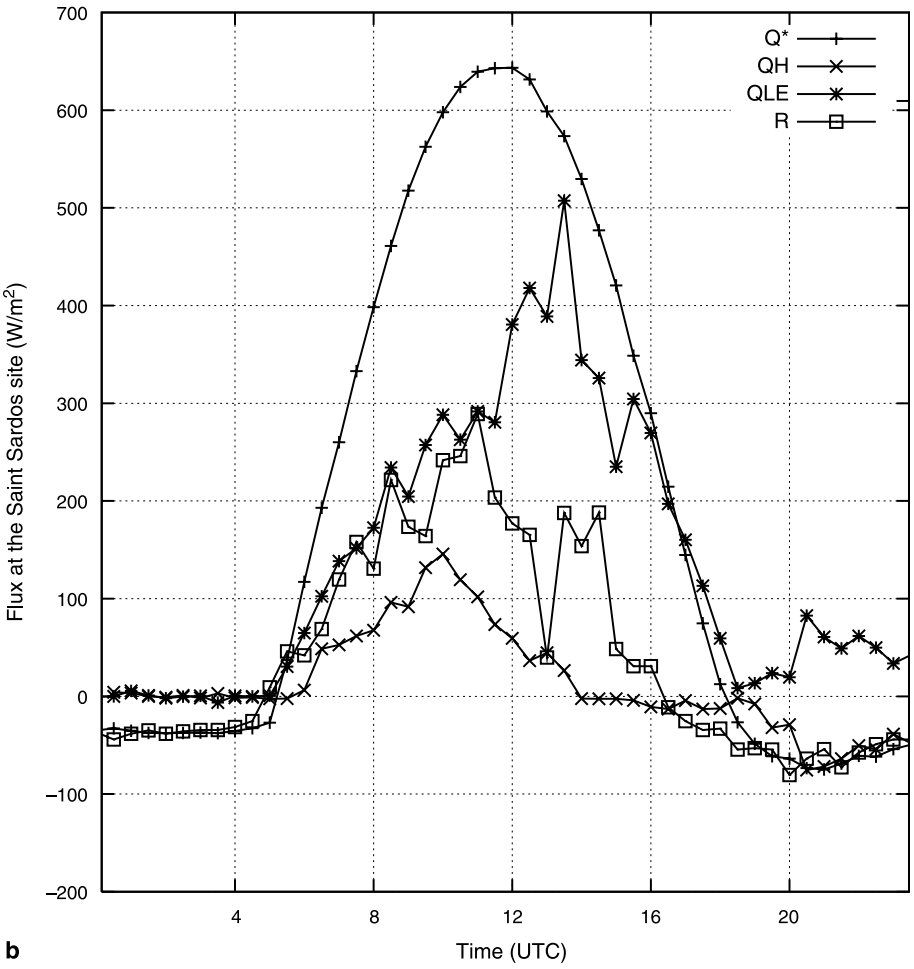

b

Fig. 3 (*continued*)

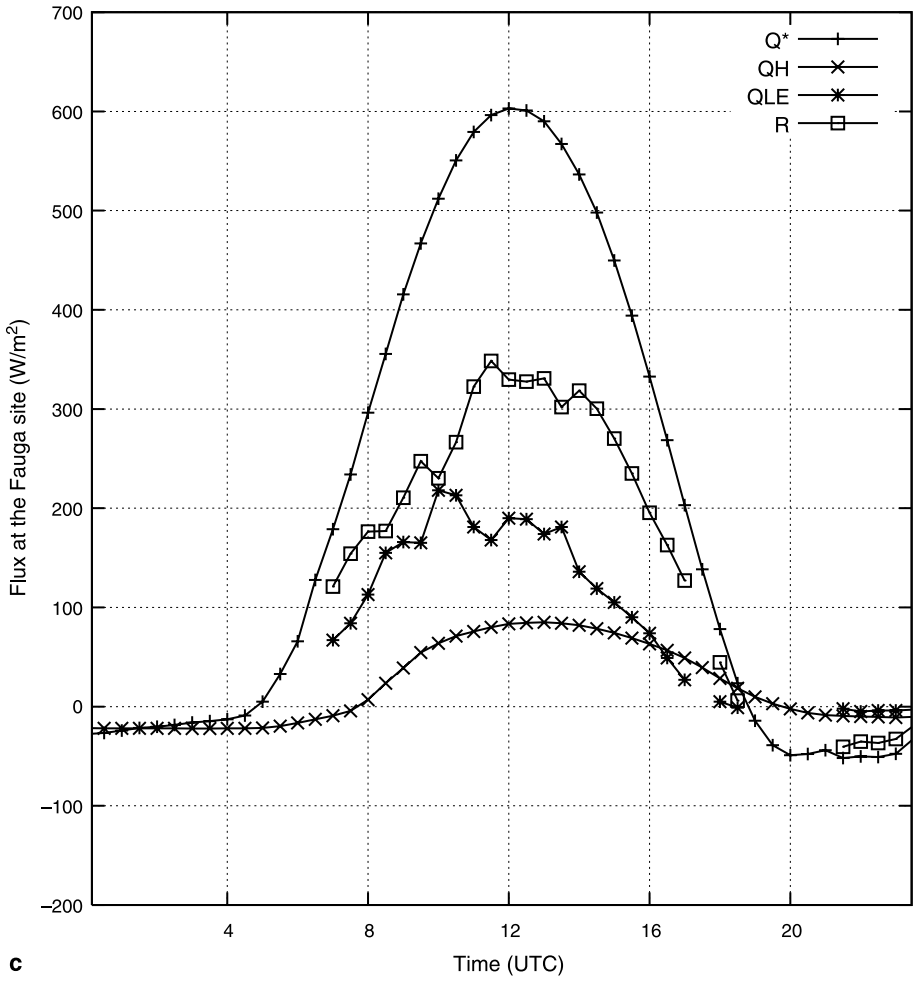

c

Fig. 3 (*continued*)

measurements at the ground stations are representative only of a small area around the station (local scale). To obtain a good representation of the diurnal cycle of the surface potential temperature and the UHI at the ''city scale'', the data from the assembly of 21 temperature and relative humidity light stations situated in the city centre and suburban areas of Toulouse were averaged according to 4 classes of urbanization (urban area, residential suburban area, non-residential suburban area and rural area, see Sect. 2).

Toulouse presents a diurnal cycle of surface potential temperature typical for an urbanized environment (Fig. 4a). In the diurnal course, urban–rural differences are strongest at night. The nocturnal cooling of the surface is slighter in the city-centre than in the rural zone, due to the liberation of the energy stored in the urban materials during the day and the reduced radiative cooling inside the urban canyons. The night from 3rd to 4th July presents a nocturnal urban heat island (Oke 1987) between 3 and 5 °C (Fig. 4b).

In the city, a large part of the solar energy is stored in the urban materials. This term is dominant during the morning. Moreover measurements were made inside of the urban canyon and are influenced by building shade, for these reasons the atmospheric heating inside of the urban canopy is delayed in comparison with the rural zones creating an urban cool island (Oke 1987). The 4th July the cool island in the city starts with the daybreak at 06.00 UTC and finish at 10.00 UTC. The morning heating delay in the city centre is significant between 08.00 and 09.00 UTC with an amplitude of 0.5 °C.

After midday, the difference of temperature between the city and the surrounding country

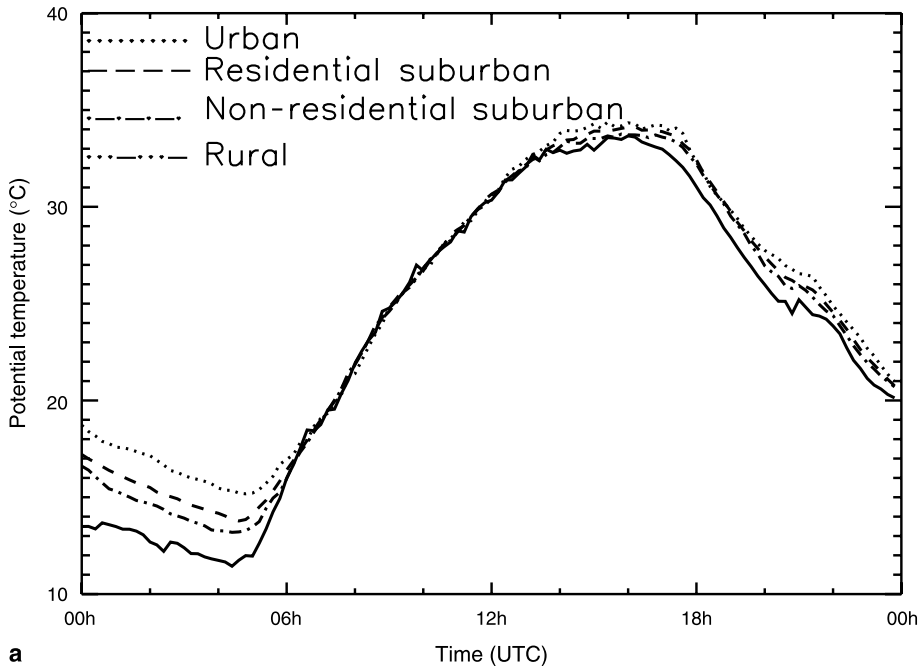

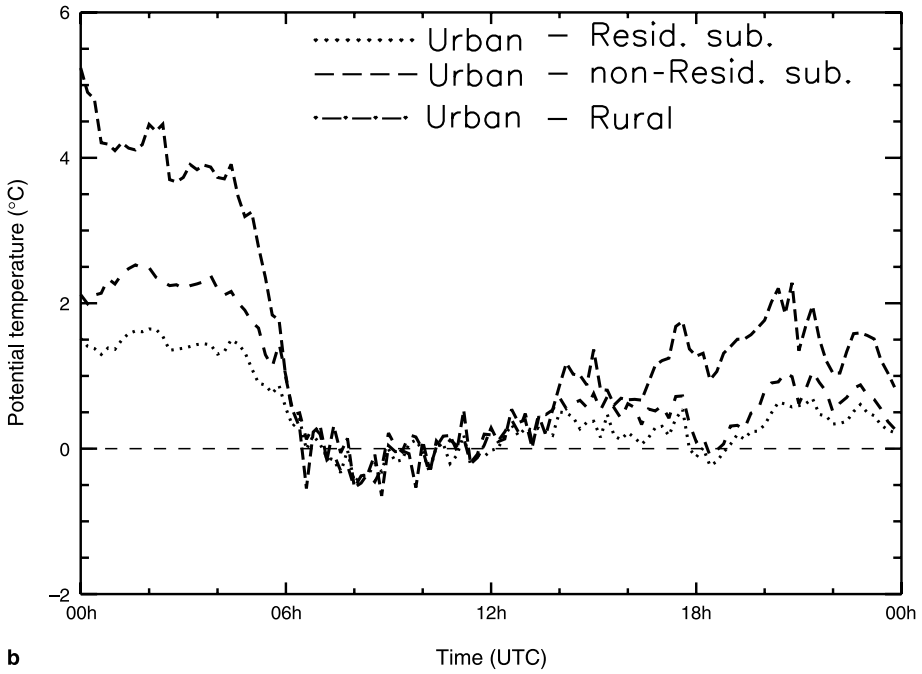

Fig. 4a, b. Temporal evolution of surface potential temperature (**a**) and urban heat island intensity (**b**) the 4th July 2004 observed at 2 m by the stations net and averaged by urbanization class

becomes positive creating a weak heat island of 1 to 1.5 °C amplitude. In average, the temperature reaches its maximum in the rural (33 °C) and urbanized zones (34 °C) at the same approximate time, i.e. 15.00 UTC. The potential temperature starts to diminish in the rural area at 16.00 UTC and in the urbanized area at 18.00 UTC. This diurnal heat island is an important element for the urban-breeze generation and for its persistence during this day.

5. The Urban-breeze circulation

5.1 Vertical structure of the ABL

For our case study, i.e. anticyclonic summer situation in a flat continental area, the vertical diurnal development of the convective ABL is mainly driven by the ground heating. All morning long, the air was warmed and homogenized by turbulence. In the first hours after dawn, this

heating was slower in the city centre than in the rural zone creating the cool island cited formerly.

At 13.00 UTC, the vertical structure is the following:

The vertical profiles of potential temperature from the radio sounding at the urban and rural (Merville) sites (Fig. 5) exhibit an unstable boundary layer, with a first inversion of temperature at the height of 1000 m over the rural zone and of 1100 m over the city, corresponding to the layer where the wind turns from SE to NW (Fig. 2). The rural site (Merville) is situated leeward of the city up to this level and is influenced by the urban UHI which is advected toward north-west (Fig. 7a). From 10.00 UTC on, the heating of the city centre boundary layer has been faster than at the Merville site. The atmospheric column over the city is 1 °C warmer than the column over the rural site.

The top of ABL, defined as the entrainment zone top height, is approximately at 1600–1700 m of height from the ground level:

– In the temperature profile from the RS, it corresponds to the summit of the second temperature inversion.
– From the aircraft measurements, it can be inferred that the ABL top is below 1750 m since from this flight level on, there is no turbulence signal on temperature time series. Moreover, given the weak turbulent signal recorded during flight P3 (Fig. 6b), it is deduced that the 1650 m level is in the entrainment zone (reached by only a few thermal updrafts penetrating through the free atmosphere from the convective mixed layer).
– The measurements from the UHF radar (Fig. 2) show a perturbation on the large scale wind field up to 2000 m and the radar reflectivity situate this transition layer at 1700 m (yellow colour).

5.2 Identification of the urban-breeze circulation by the analysis of the aircraft data

Aircraft flew twice during this day providing an horizontal appreciation of the phenomenon. In this study we will focus on the afternoon flight performed between 12.08 and 15.26 UTC.

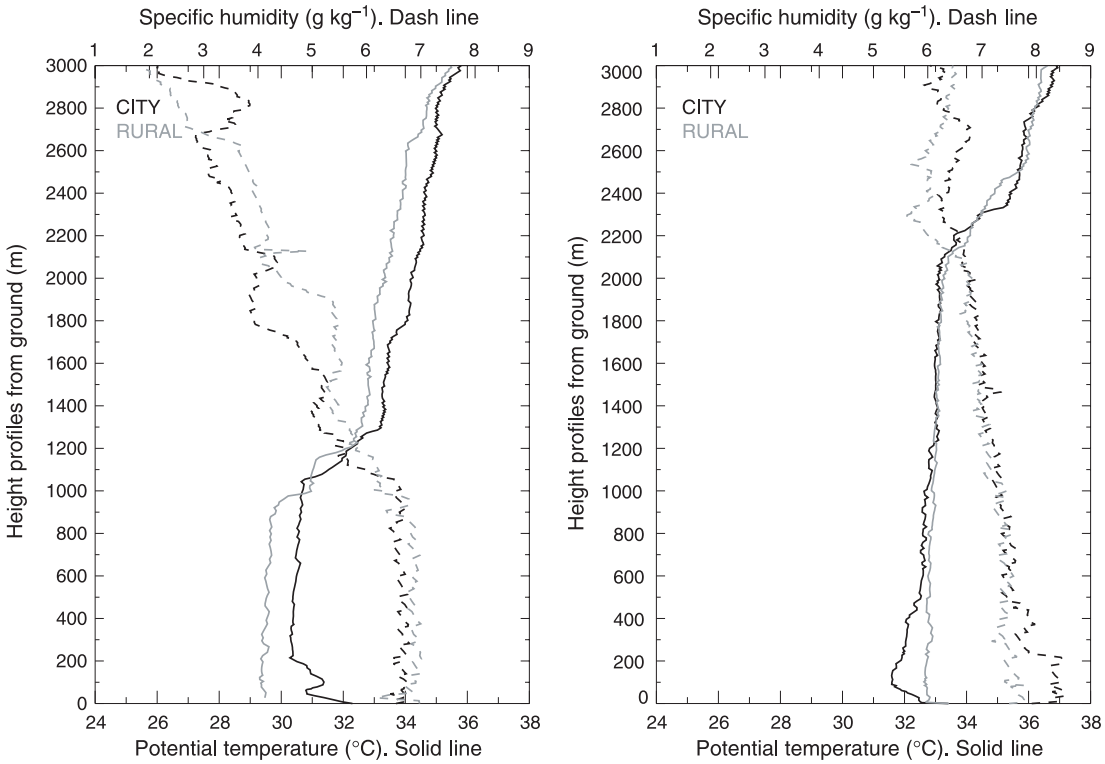

Fig. 5. Vertical profiles of potential temperature and specific humidity from radio sounding launched at the city centre and at the rural site. The 4th July 2004 at 13.00 UTC (left) and 18.00 UTC (right)

5.2.1 Flight description

The flight was divided in 3 main legs:

– P1 (13.33–14.15 UTC): flight leg crossing the urban area and its surrounding country along a NW–SE axis at 350 m.
– P2 (14.51–15.20 UTC): flight leg focused on the urban area at 1100 m
– P3 (12.32–13.11 UTC): flight leg crossing the area from the NW–SE axis at 1650 m.

The aircraft legs are superposed over a map of Toulouse and its surroundings (Fig. 7a, b and c).

5.2.2 Potential temperature analysis

The perturbation on potential temperature created by the city (anomaly) is calculated for each flight leg. We consider that a flight leg is in the ABL when the temperature signal is dominated by the high frequency created by the turbulent motions (Fig. 6b). If the flight leg is sufficiently long, the signal of the diurnal evolution is also visible. A flight leg situated outside of the ABL has a weaker frequency variation and its diurnal cycle is negligible.

The anomaly of potential temperature field is calculated taking into account the above-mentioned characteristics. For the flight legs at 350 and 1100 m (inside the mixing layer), the diurnal trend of the temperature is removed using a least-square fit function. The tendency of 2 °C h^{-1} at 350 m and 1 °C h^{-1} at 1100 m compares well with the diurnal trend of temperature estimated from the surface network (temperature averaged by zones) during the same period (1.5 °C h^{-1}).

The flight leg P1 shows a clear diurnal evolution of 1.5 °C and a relative maximum (Fig. 6b) corresponding to the passage above the city. When this trend of 1.5 °C is removed from the temperature data, the result is a 1 °C amplitude heat island over the city (Fig. 7a) in agreement with the radio soundings at 13.00 UTC.

The same treatment is applied for the P2, a trend of 0.5 °C being removed from the temperature data. In this flight leg the anomaly is off-centre, to the north-west (to leeward of the centre) and its intensity is slightly weaker (0.5 °C) (Fig. 7b).

In the flight leg P3 (1650 m of height), corresponding at this hour with the entrainment zone (Figs. 2 and 6), a large scale horizontal gradient (NW–SE) of temperature is observed by the aircraft (Fig. 6b) and the radio sounding (Fig. 5a, from 1200 m of height). A mean of the temperature field over the city is used to calculate the perturbation created by the city at this height (Fig. 7c). The temperature anomaly centred over the city is only visible in a little fraction of the flight leg (12.50–12.53 UTC in Fig. 6b where the aircraft encounters a more turbulent zone between 42.5 and 43.65 of latitude in Fig. 7c) suggesting that this level is still affected by the presence of the city by means of stronger updraft motions due to the enhanced sensible heat flux.

Note that in the numerical study of this case (Hidalgo et al. 2008) the large scale horizontal

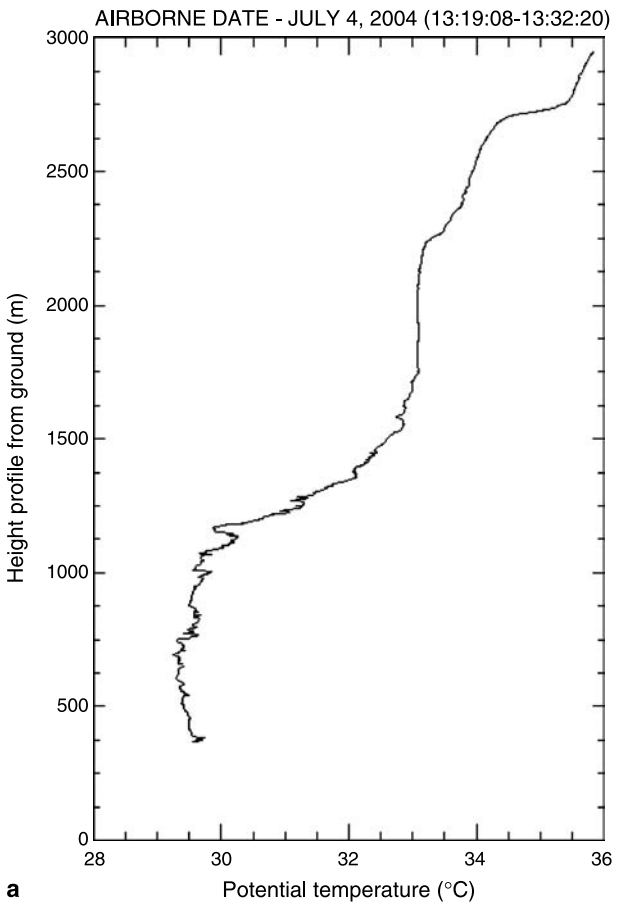

Fig. 6a, b. Vertical profile of potential temperature from the airborne sounding in the rural zone at 13.20 UTC (**a**). Temporal evolution of potential temperature observed by the aircraft (**b**) at height of 350 m, 1100 m and 1650 m. And a vertical profile of potential temperature from 3000 m to 1950 m. The black strip indicates when the aircraft over flies Toulouse

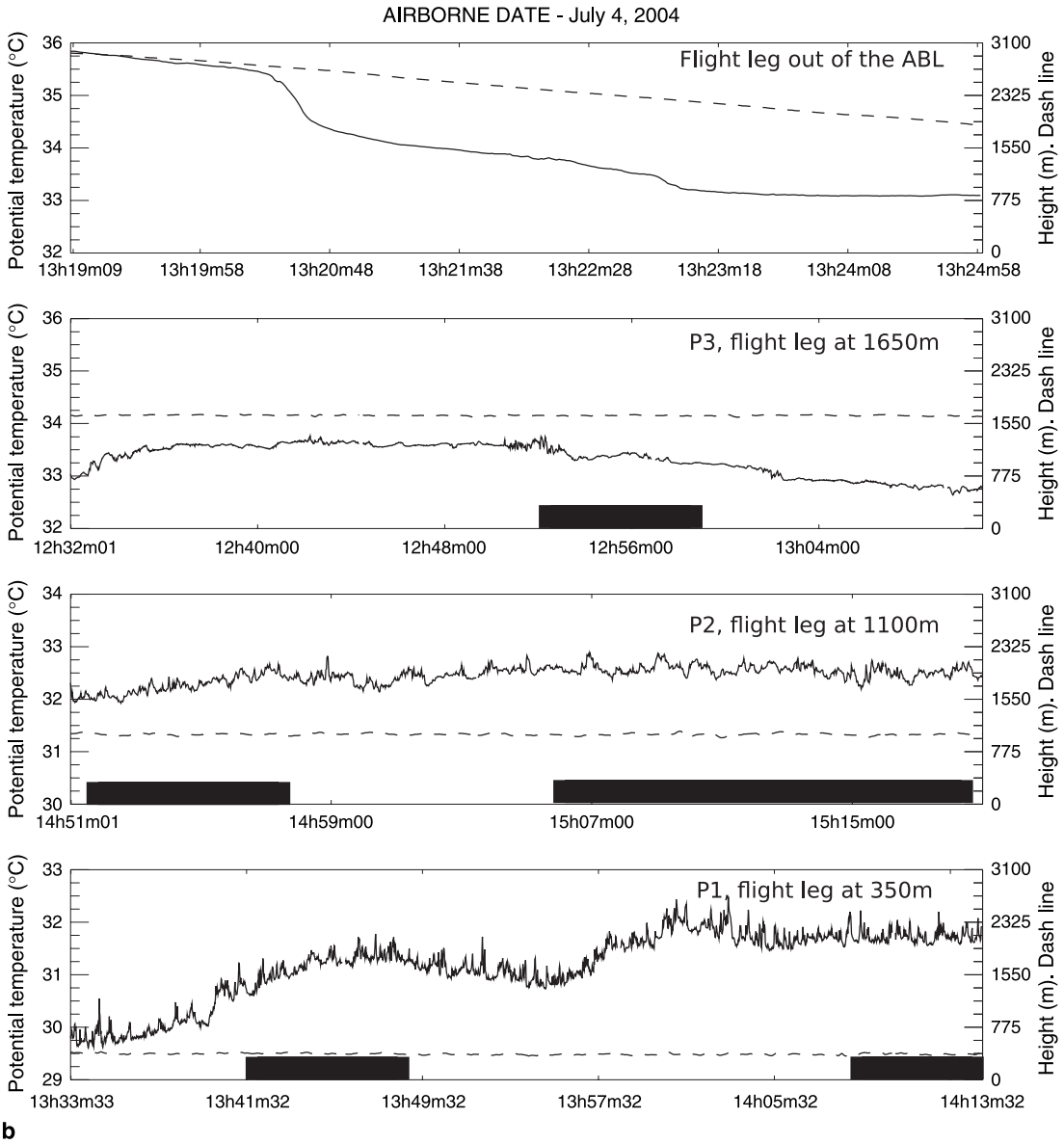

b

Fig. 6 (*continued*)

gradient of temperature oriented in a NW–SE axis and the higher boundary layer over the city due to the updraft motions are confirmed and analysed.

5.2.3 Wind field analysis

The wind field measured by the aircraft flight allows to study the dynamics in the ABL, as these data provide a horizontal view of movements at three heights. The mean wind field provided by the flight leg at 350 m (Fig. 8a) shows a weak south-easterly flow with a wind velocity smaller than 5 m s^{-1} over the urban area and even more to leeward of the city. The flight leg at 1650 m (Fig. 8c) is submitted to a stronger westerly-north-westerly flow, which creates at 1100 m a transition layer between the two regions with a weak wind (Fig. 8b).

At this hour, the perturbation created by the city in the mean wind field is still small compared to the magnitude of the wind, so this is not directly visible in the mean field. As for the potential temperature, the anomaly is calculated for each flight leg. The wind anomalies are computed excluding the zones with strong swerves of the aircraft. Furthermore, the synoptic trend for each leg, even if small, is linearly

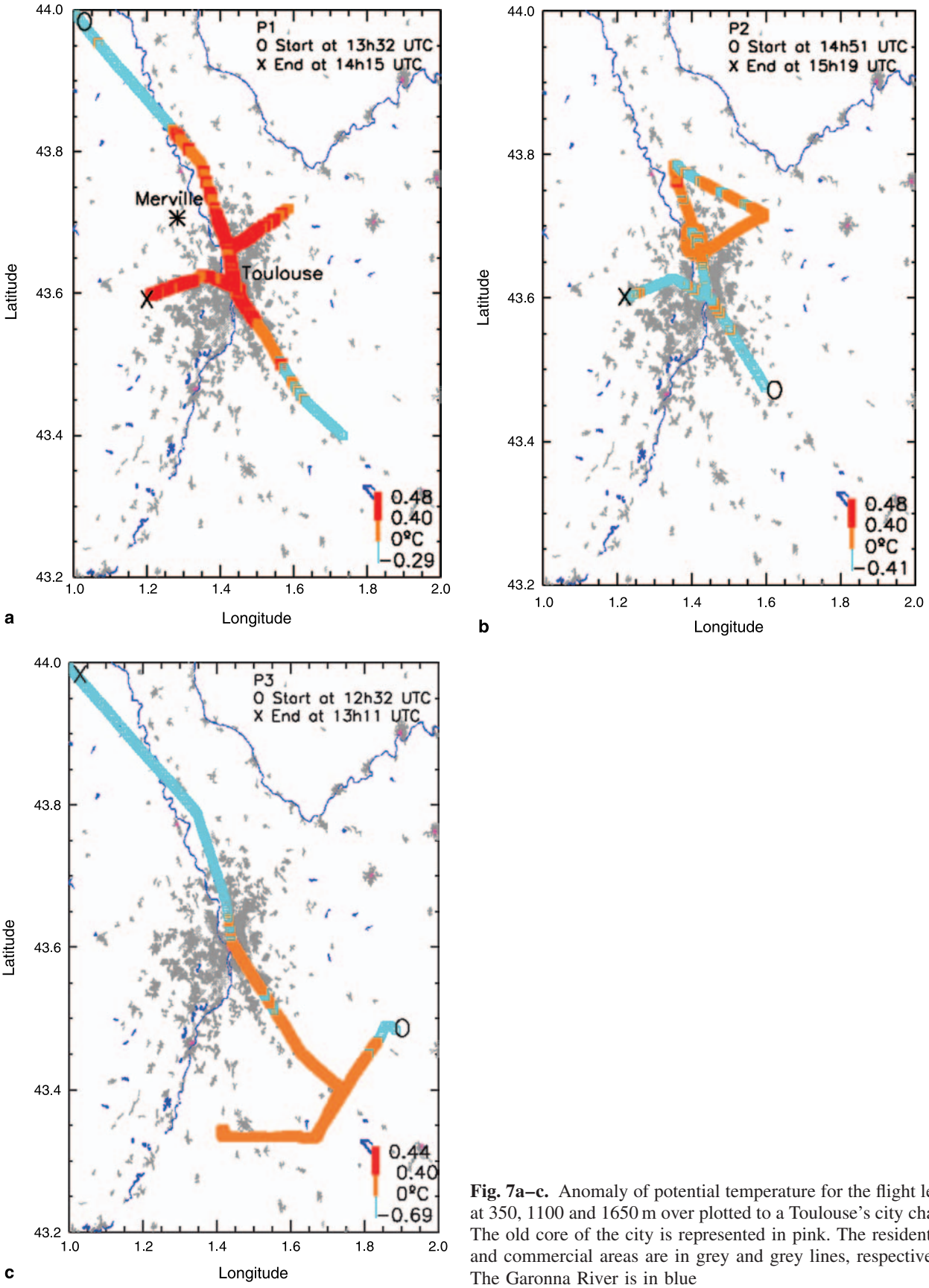

Fig. 7a–c. Anomaly of potential temperature for the flight legs at 350, 1100 and 1650 m over plotted to a Toulouse's city chart. The old core of the city is represented in pink. The residential and commercial areas are in grey and grey lines, respectively. The Garonna River is in blue

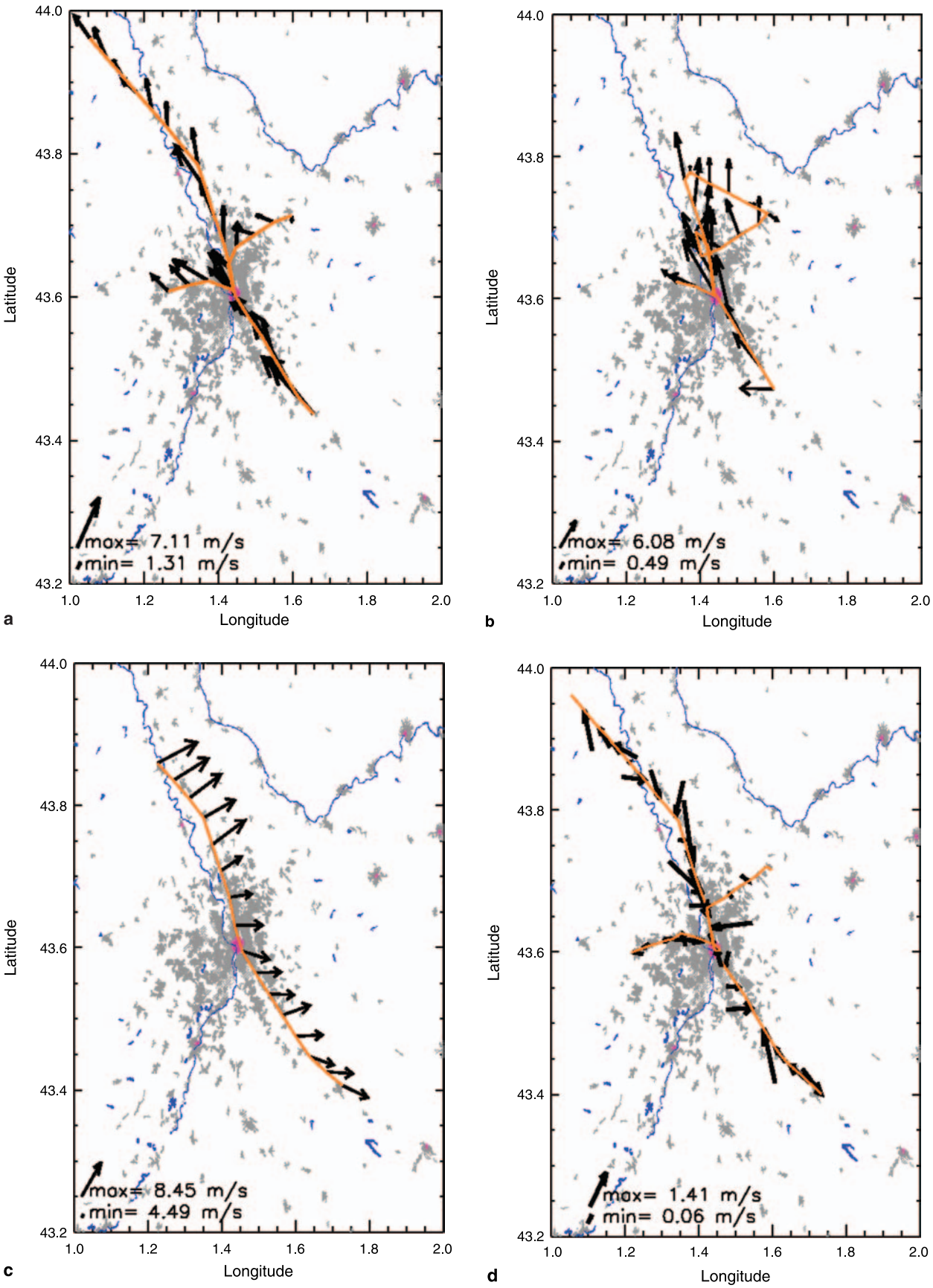

Fig. 8a–f. Mean wind field (**a**, **b**, **c**) and its anomaly (**d**, **e**, **f**), for the flight legs at 350, 1100 and 1650 m over plotted to a Toulouse's city chart. The old core of the city is represented in pink. The residential and commercial areas are in grey and grey lines respectively. The Garonna River is in blue

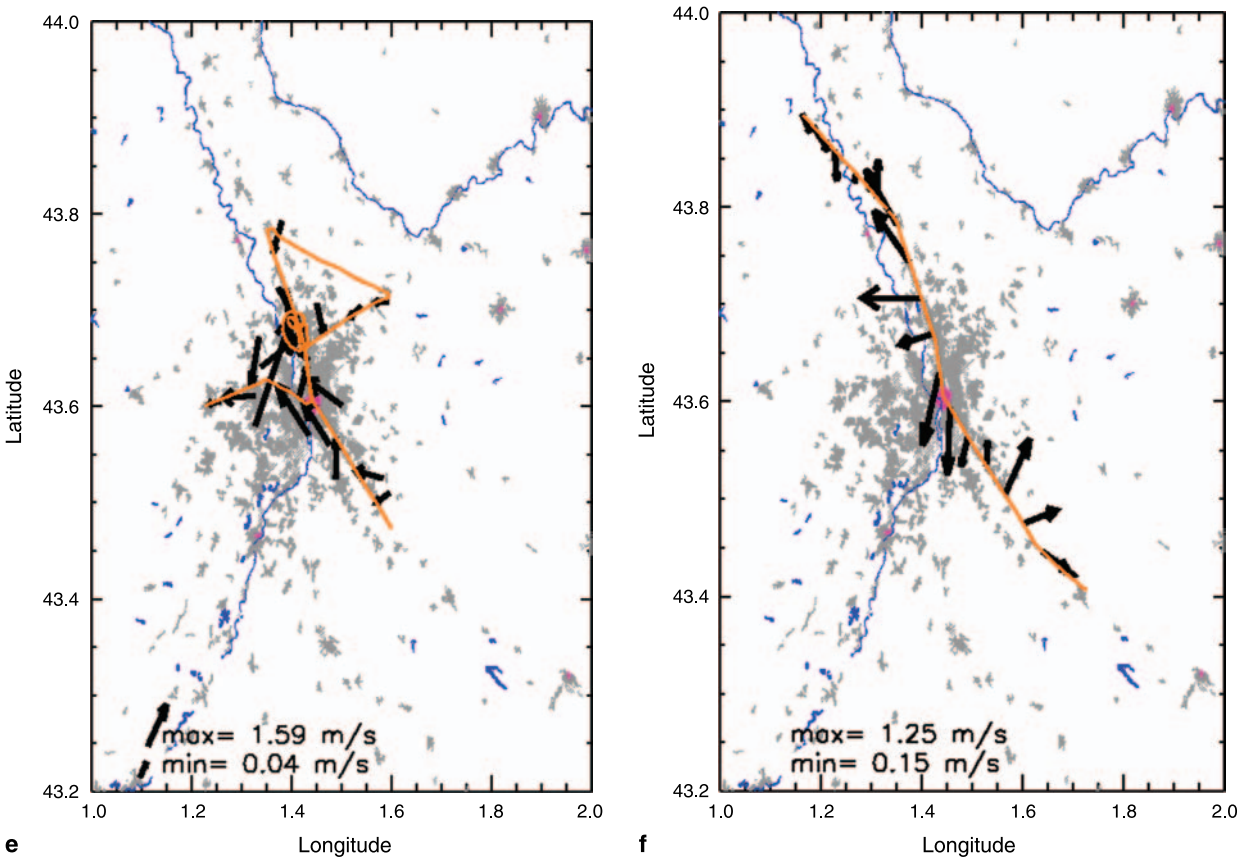

Fig. 8 (*continued*)

removed in order to focus on the perturbation due to the city. The result is averaged over 60 s in order to filter small scale turbulence. The aircraft speed being 72 m s^{-1} allows to take into account only the motions at scales larger than 4 km.

At the lowest levels (350 m, Fig. 8d and 1100 m, Fig. 8e) taking into account the UHI aforementioned a convergent flow towards the city centre is attended. This is true for P1 where clear convergence of 1–1.5 m s^{-1} is highlighted at 350 m with a horizontal extension of approximately 25 km (from 43.55 to 43.75 of latitude). The P2 is situated in the transition layer between the South-Easterly and North-westerly flows, due to weaker anomalies of temperature and wind, the result is more difficult to interpret in terms of convergence to the city centre at 1100 m of height. Even though the urban-breeze is driven by the SEB, vertical observations of the ABL structure are important to describe the horizontal transport in the lower layers.

At 1650 m (Fig. 8f), a well marked divergence (the flow goes from the city centre to the outskirts) reaching 2 m s^{-1} is developed over the city. Its extension is about 30 km (from 43.55 to 43.8 of latitude) off-centre to the North-West. Because the flight leg at 1650 m is in the thermal inversion, this shows that the wind perturbation due to the city extends to the entrainment zone.

6. Time-evolution of the breeze

At the end of the afternoon, the ABL stops its vertical development and its height becomes stationary reaching a maximal height of 2200 m observed at 18.00 UTC in the city centre and 2000 m at Merville site (Fig. 5b). At this hour the horizontal gradient of temperature between the city centre and the rural site has vanished, and the city centre is now even cooler and moister in a layer from the surface to 400 m of height. Fresh air is transported by the South-Easterly flow from the rural zone situated upwind (Fig. 9). This

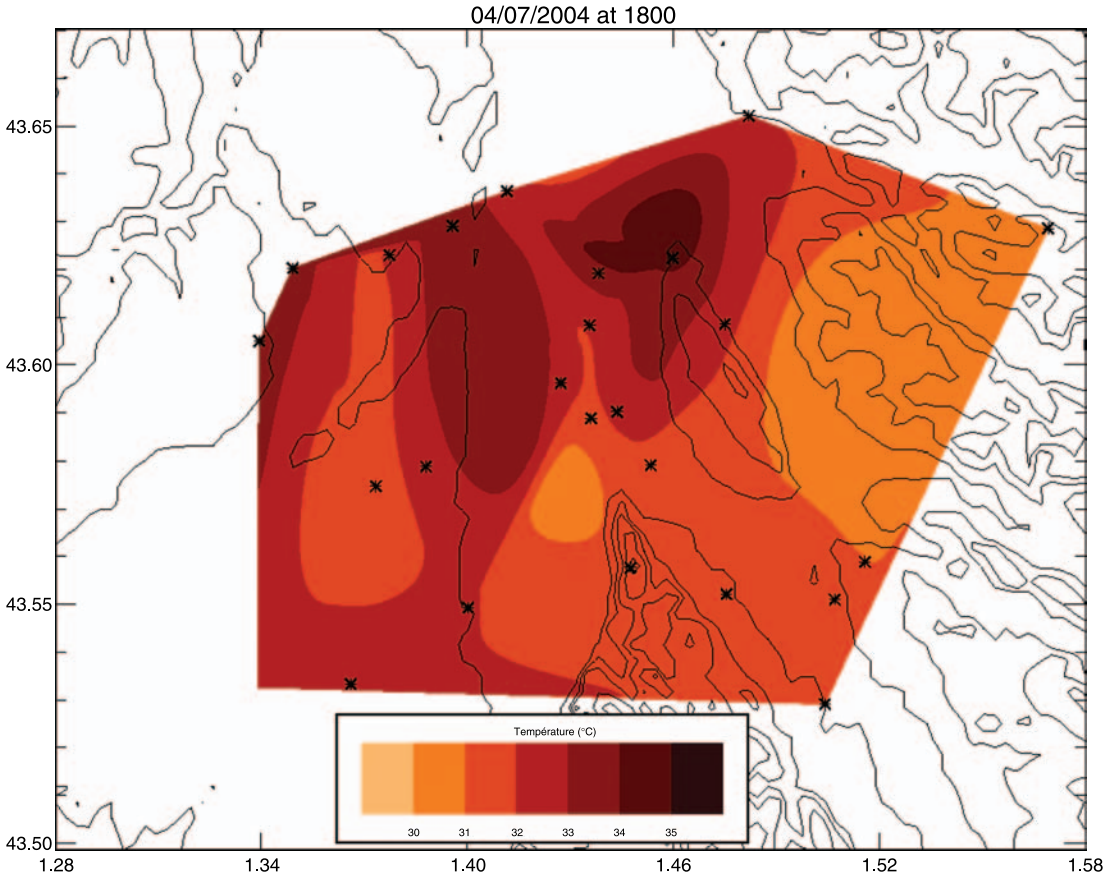

Fig. 9. Horizontal field of potential temperature measured by the micro-meteorological stations, the 4th July 2004 at 18.00 UTC

air mass is warmed over the city before reaching Merville.

The centre of the breeze is advected downstream of the city where the UHI is now located. A south-easterly flow in surface and a north-westerly flow at upper-levels is identified at the city centre in the RS of 18.00 UTC (Fig. 10). This configuration indicates a convergent branch from the rural site (Merville, situated in the north-west) to the city at 250 m of height and a divergent branch from the city centre to the rural from 1500 m upwards. The urban-breeze circulation of 5–6 m s^{-1} intensity, probably enhanced by the continuous strong surface heating of the city, is then able to dominate the flow pattern at 18.00 UTC.

7. Conclusions

This study is focused on the IOP5 of the CAPITOUL experiment. Its main objective is to analyse an urban-breeze situation observed over the city of Toulouse (South-West of France) the 4th July, 2004. The meteorological conditions and the thermo-dynamical properties of the ABL were described using ground stations, wind profilers, radio soundings and aircraft data.

The synoptic situation of this day is favourable to the development of an urban-breeze circulation. This was a high insulated situation, the maximum net radiation being close to 650 W m^{-2}. The maximum of temperature in the city centre reached 34 °C during this day. Moreover, a weak south-easterly flow in surface and a north-westerly flow at upper-levels created a region of a weak flow in the transition layer between the two regimes.

Typical features of urbanized areas described in the literature were found for this period. A nocturnal urban heat island of +5 °C amplitude and a cool island of −1 °C amplitude in the early morning were described in Sect. 3. Due to re-

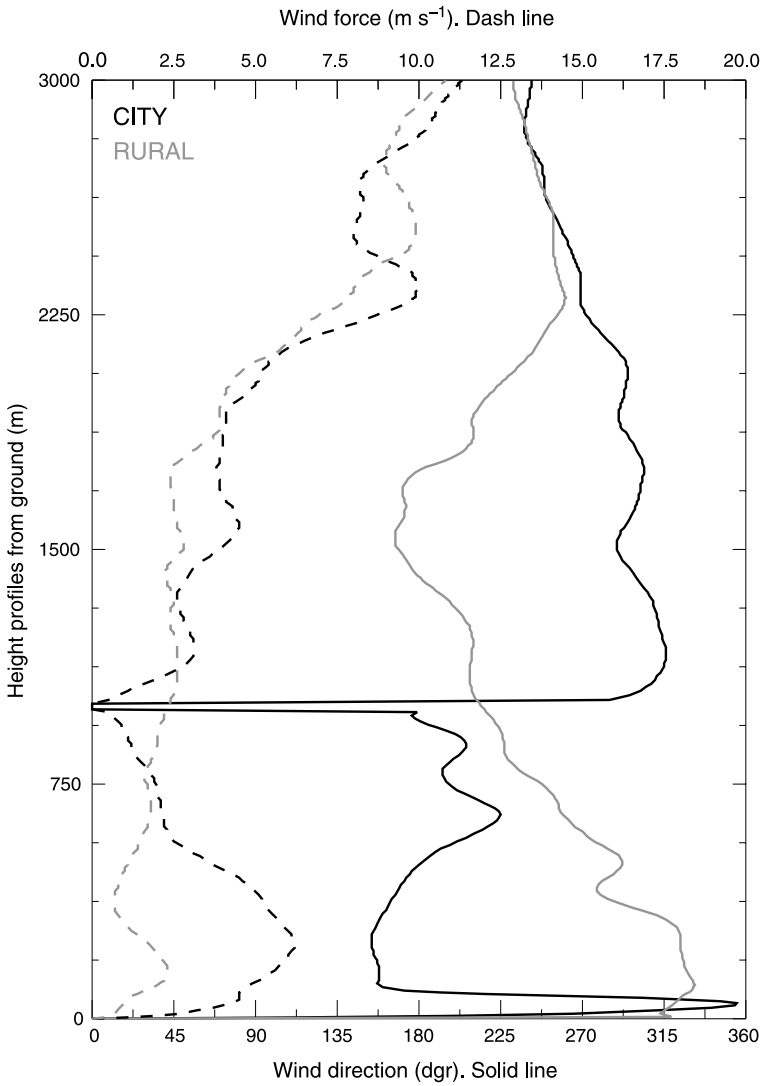

Fig. 10. Vertical profiles of wind force and wind direction from radio sounding launched at the city centre and at the rural site. The 4th July 2004 at 18.00 UTC

duced daytime evapotranspiration in the urban area, the sensible heat flux was during the afternoon approximately 250 W m^{-2} larger than in the countryside. This is the important feature of the Surface Energy Balance leading to an urban breeze.

This study shows the relative roles of the SEB components and the ABL structure for the development of the low-level airflow convergence towards the city. Even though the urban-breeze is driven by the SEB, surface measurements should go with vertical observations of the ABL structure to properly describe the horizontal transport in the lower layers.

The daytime +1 °C heat island centred in the city centre at 350 m of height and advected to leeward of the city at 1100 m of height is associated to the urban-breeze generation. The gradient of temperature starts at 12.00 UTC. The breeze observed by the aircraft between 12.30 to 15.20 UTC is composed of:

- Near surface convergence towards the city with an intensity of 1–2 m s^{-1} and with a horizontal extension in the axis SE–NW which is 2–3 times bigger than the size of the city.
- Divergent return in upper levels at the top of the ABL, reaching 2 m s^{-1} at 13.00 UTC.

The urban-breeze circulation grows in intensity during the afternoon and is able to dominate the flow pattern at 18.00 UTC.

This phenomenon has already been simulated by Lemonsu and Masson (2002) for Paris (France). The airborne measurements during the CAPITOUL campaign combined with the ground stations, wind profilers and radio soundings data, tends to demonstrate experimentally the existence of this kind of breeze in inland

urbanized areas. This urban breeze episode was simulated with the MESONH model (Lafore et al. 1998) and presented in a companion paper by Hidalgo et al. (2008).

Acknowledgements

This research was performed with a PhD grant co-founded by the French National Centre of Meteorological Research and the FAO9 team of the University of Vigo in Spain (Education and Science Ministry; DIMPRE project, Ref: CGL2004-05187-C03-02/CLI). The authors would like to thanks the kindly help of the instrumentation team in special to Arnaud Mequignon (CNRM/GMEI/TRAMM) for help in the treatment of aircraft data, key part of this study.

We are also grateful to Sue Grimmond and two anonymous reviewers who offered a critical review that significantly enhanced our appreciation of the problem treated here.

References

Atkinson BW (1981) Meso-scale atmospheric circulations. Academic Press, 195 pp

Augustin P, Delbarre H, Lohou F, Campistron B, Puygrenier V, Cachier H, Lombardo T (2006) Investigation of local meteorological events and their relationship with ozone and aerosols during an ESCOMPTE photochemical episode. Ann Geophys 24: 2809–22

Changnon SA (1981) METROMEX: a review summary. Monograph, No. 40, Vol. 18. American Meteorlogical Society, Boston, USA

Christen A, Vogt R (2004) Energy and radiation balance of a central European city. Int J Climatol 24: 1395–421

Eliasson I, Svensson M (2003) Spatial air temperatures, street geometry and land use. Atmos Environ 30: 379–92

Feliks Y (1994) An analytical model of the diurnal oscillation of the inversion base due to the sea-breeze. J Atmos Sci 51: 991–8

Finkele K, Hacker JM, Krauss H, Scott RA (1995) A complete sea breeze circulation cell derived from aircraft observations. Bound Layer Meteorol 73: 299–317

Fisher E (1960) An observational study of the sea breeze. J Meteorol 17: 645–60

Grimmond CSB, Oke TR (1999) Heat storage in urban areas: local-scale observations and evaluation of a simple model. J Appl Meteorol 38: 922–40

Hidalgo J, Masson V, Pigeon G (2008) Urban-breeze circulation during the CAPITOUL experiment: numerical approach. Meteorol Atmos Phys (submitted)

Lafore JP et al. (1998) The Meso-NH atmospheric simulation system. Part I: adiabatic formulation and control simulations. Ann Geophys 16: 90–109

Lemonsu A, Masson V (2002) Simulation of a summer urban breeze over Paris. Bound Layer Meteor 104: 463–90

Lemonsu A, Grimmond CSB, Masson V (2004) Modelling the surface energy balance of an old Mediterranean city core. J Appl Meteorol 43: 312–27

Lemonsu A, Bastin S, Masson V, Drobinski P (2006a) Stratification of the urban boundary layer of marseille under sea-breeze condition: joint analysis of Doppler lidar and numerical simulations. Bound Layer Meteor 118: 477–501

Lemonsu A, Masson V, Pigeon G, Moppert C (2006b) Sea-town interactions over marseille: 3d urban boundary layer and thermodinamical field near the surface. Theor Appl Climatol 84: 171–8

Masson V, Gomes L, Pigeon G, Liousse C, Pont V, Lagouarde JP, Voogt J, Salmond J, Oke TR, Hidalgo J, Legain D, Garrouste O, Lac C, Connan O, Briottet X, Lachérade S, Tulet P (2008) The Canopy and Aerosol Particles Interactions in TOulouse Urban Layer (CAPITOUL) experiment. Meteorol Atmos Phys 102: 135–57

Nakane H, Sasano Y (1986) Structure of a sea breeze front revealed by scanning lidar observation. J Meteorol Soc Jpn 64: 787–92

Niino H (1987) The linear theory of land and sea breeze circulation. J Meteorol Soc Jpn 65: 901–20

Oke T (2005) Towards better scientific communication in urban climate. Theor Appl Climatol, 84: 179–90

Oke TR (1981) Canyon geometry and the nocturnal urban heat island: comparison of scale model and field observations. Int J Climatol 1: 237–54

Oke TR (ed) (1987) Boundary layer climates. Methuen, London & York

Oke TR (1988) The urban energy balance. Prog Phys Geogr 12: 471–508

Oke TR, Sproken-Smith R, Jàuregu E, Grimmond S (1999) The energy balance of centrel Mexico City during the dry season. Atmos Environ 33: 3919–30

Pigeon G, Lemonsu A, Barrié J, Durand P, Masson V (2006) Urban thermodynamic island in a Coastal City analised from an optimized surface network. Bound Layer Meteor 232: 1–37

Pigeon G, Lemonsu A, Grimmond CSB, Durand P, Thouron O, Masson V (2007a) Divergence of turbulent fluxes in the surface layer: case of a coastal city. Bound Layer Meteor 124: 269–90

Pigeon G, Legain D, Durand P, Masson V (2007b) Anthropogenic heat release in an old European city (Toulouse, France). Int J Climatol 27: 1969–81

Rotunno R (1983) On the linear theory of the land sea breeze. J Atmos Sci 40: 1999–2009

Shepherd JM (2005) A review of current investigations of urban-induced rainfall and recommendations for the future. Earth Interactions 9: 1–27

Unger J, Sümeghy Z, Gulyás A, Bottayán Z, Mucsi L (2001) Land-use and meteorological aspects of the urban heat island. Meteorol Appl 8: 189–94

Walsh J (1974) Sea breeze theory and application. J Atmos Sci 31: 2012–26

White J, Eaton F, Auer A (1978) The net radiation budget of the St. Louis metropolitan area. J Appl Meteorol 17: 593–9

Wilson K, Goldstein A, Falge E, Aubinet M, Baldocchi D, Berbigier P, Bernhofer C, Ceulemans R, Dolman H, Field C, Grelle A, Ibrom A, Law B, Kowalski A, Meyers T, Moncrieff J, Monson R, Oechel W, Tenhunen J, Valentini R, Verma S (2002) Energy balance closure at FLUXNET sites, Agric Forest Meteorol 113: 223–43

Wong KK, Dirks RA (1978) Mesoscale perturbations on airflow in the urban mixing layer. Amer Meteorol Soc 17: 677–88